Supporting Information

Structure of the Alk1 extracellular domain and characterization of its BMP binding properties

Pardeep Mahlawat, Udayar Ilangovan, Tanuka Biswas, LuZhe Sun, and Andrew P. Hinck

Figure 1. ESI-TOF mass spectra of Alk1-ED and Alk3-ED. The electrospray ionization time-of-flight (ESI-TOF) mass spectra were acquired on an Agilent 6224 ESI-TOF instrument used in conjunction with an Agilent 1260 Infinity binary pump HPLC system. Shown above each peak are the observed *m/z* (average mass) and the corresponding charge state of the ion. Peaks marked with "*" are from gas-phase dimers. Deconvoluted mass spectra obtained though use of the molecular feature extractor component of the Agilent MassHunter software package are shown in the insets.

Figure 2. ^{1}H-^{15}N HSQC spectra of ^{15}N Alk1-ED and ^{15}N Alk3-ED. Spectrum of Alk1-ED was recorded at 600 MHz ^{1}H at a temperature of 32 °C. Sample buffer consisted of 25 mM sodium phosphate, 5% $^{2}H_2O$, 0.02% w/v sodium azide, pH 5.5. Spectrum of Alk3-ED was recorded at 600 MHz ^{1}H at a temperature of 25 °C. Sample buffer consisted of 25 mM sodium phosphate, 5% $^{2}H_2O$, 0.02% w/v sodium azide, pH 6.3.

Figure 3. Antagonistic potencies of Alk1-ED and Alk3-ED in a cell-based bioassay. (A) Antagonistic potency of Alk1-ED was assessed by transiently transfecting NIH-3T3 fibroblasts with a full-length Alk1 construct and then treating the cells with 200 pM BMP-9 alone or in the presence of increasing concentrations of the Alk1-ED (or Alk3-ED as a negative control). Activities were assessed by lysing the cells and analyzing 30 μg of protein by Western blotting with phosphoSmad 1/5/8 and Smad5 antibodies; a GAPDH antibody was also used to control for differences in the total amount of protein loaded. (B) Antagonistic potency of Alk3-ED was assessed as above, except by transfecting the NIH 3T3 fibroblasts with a full-length Alk3 construct (instead of Alk1) and by treating the cells with 800 pM BMP-2 (instead of 200 pM BMP-9).

Figure 4. SPR binding analysis of Alk1-ED variants to BMP-9. Sensorgrams shown represent serial two-fold dilutions of Alk1-ED variants over a BMP-9 surface. Sensorgrams shown have been corrected for background binding to a surface with no coupled ligand and as well referenced against blank buffer injections. Disassociation constants (K_d) were obtained by fitting the equilibrium binding response (R_{eq}) as a function of injected receptor concentration to $R_{eq} = (R_{max} \times [R]/K_d + [R])$ (not shown). All experiments were repeated two to three times, except N50A, R53D, and L55Q, which were only measured once.

Figure 5. One-dimensional ^{1}H NMR spectra of Alk1-ED variants. Spectra were recorded at 500 MHz at 32 °C using a WATERGATE solvent suppression scheme [Piotto, Saudek, & Sklenar, J. Biomol. NMR

2:661-665]. Sample buffer consisted of 25 mM sodium phosphate, 5% $^{2}H_2O$, 0.02% w/v sodium azide, pH 5.5.

Figure 6. One-dimensional ^{1}H NMR spectra of Alk3-ED variants. Spectra were recorded at 500 MHz at 25 °C using a WATERGATE solvent suppression scheme [Piotto, Saudek, & Sklenar (1992) J. Biomol. NMR 2:661-665]. Sample buffer consisted of 25 mM sodium phosphate, 5% $^{2}H_2O$, 0.02% w/v sodium azide, pH 6.3.

Figure 7. Sequence alignment of the ectodomain of several known mammalian Alk1 sequences. Sequences were aligned using the program ClustalW [Larkin, et. al (2007) Bioinformatics, 23:2947-2948]. Arg53 is highlighted in cyan and Glu54 and Leu55 are highlighted in red.

Figure 8. Structure of the Alk3:BMP-2 complex and alternative Alk3:BMP-2 complex in which Alk3 is bound in an Alk1-like manner. (A) Structure of Alk3 (blue) bound to BMP-2 (yellow) as determined using crystallography [Kirsch, et. al (2000) Nat. Struct. Biol, 7:492-496] (left) or by positioning Alk3 as Alk1 is positioned onto BMP-9 in the structure of the Alk1:BMP-9 complex determined using RosettaDock (right). Extent of yellow shading on the ligand surface and yellow color on the receptor ribbon corresponds to the severity of the clashes. (B) Stereoview of Alk3:BMP-2 complex in which Alk3 is bound in Alk1-like manner (same as panel A, right). Extent of yellow shading on BMP-2 and yellow color on Alk3 corresponds to the severity of the clashes. Sidechains of Alk3 (blue labels) and BMP-2 (brown labels) that clash are shown. Clashes depicted in panel A were calculated using the clash function within the program Chimera [Pettersen, et. al (2004) J. Comput. Chem. 25:1605-1612].

Fig. 1

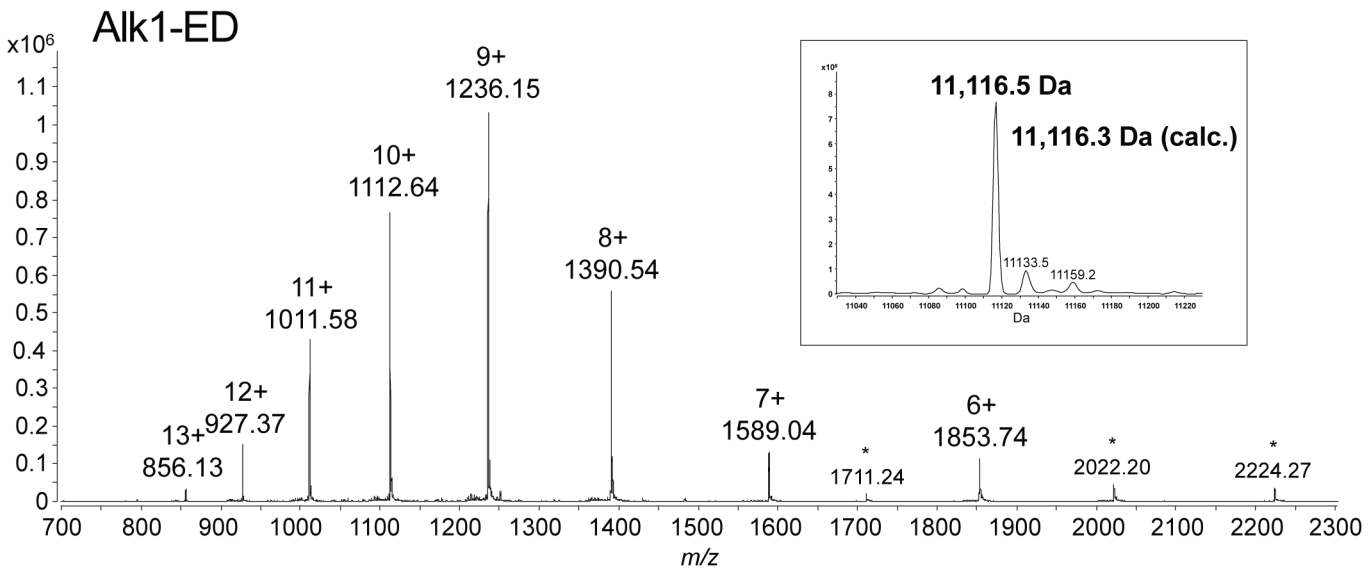
Alk1-ED
x10^6
9+
1236.15
10+
1112.64
8+
1390.54
11+
1011.58
12+
927.37
13+
856.13
7+
1589.04
6+
1853.74
*
1711.24
*
2022.20
*
2224.27
11,116.5 Da
11,116.3 Da (calc.)
11133.5
11159.2
Da
m/z

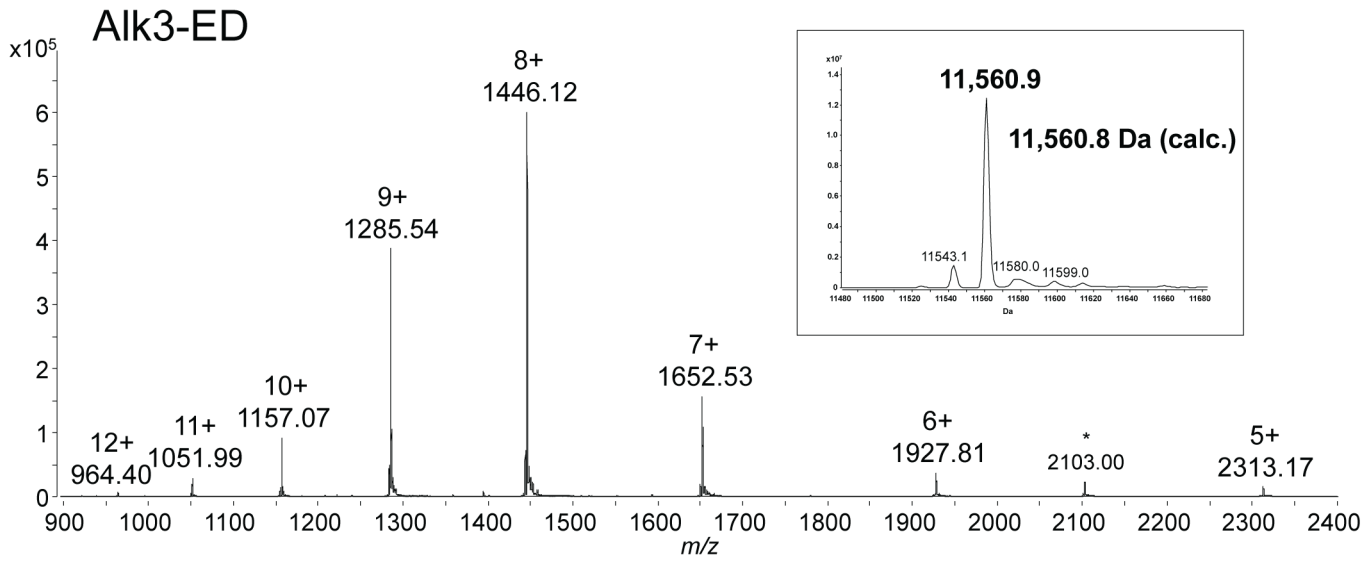
Alk3-ED
x10^5
8+
1446.12
9+
1285.54
7+
1652.53
10+
1157.07
11+
1051.99
12+
964.40
6+
1927.81
*
2103.00
5+
2313.17
11,560.9
11,560.8 Da (calc.)
11543.1
11580.0
11599.0
Da
m/z

Fig. 2

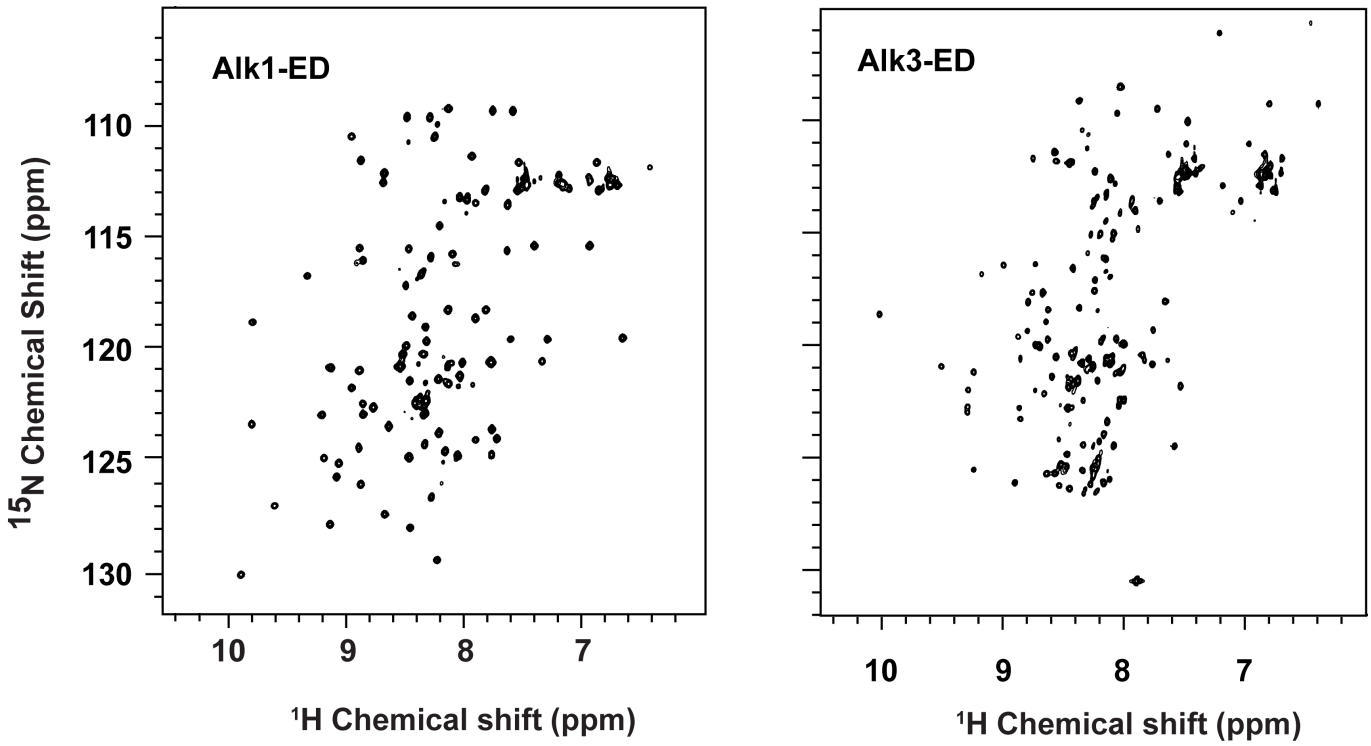
Alk1-ED
110
115
120
125
130
^{15}N Chemical Shift (ppm)
10
9
8
7
^{1}H Chemical shift (ppm)
Alk3-ED
10
9
8
7
^{1}H Chemical shift (ppm)

Fig. 3.

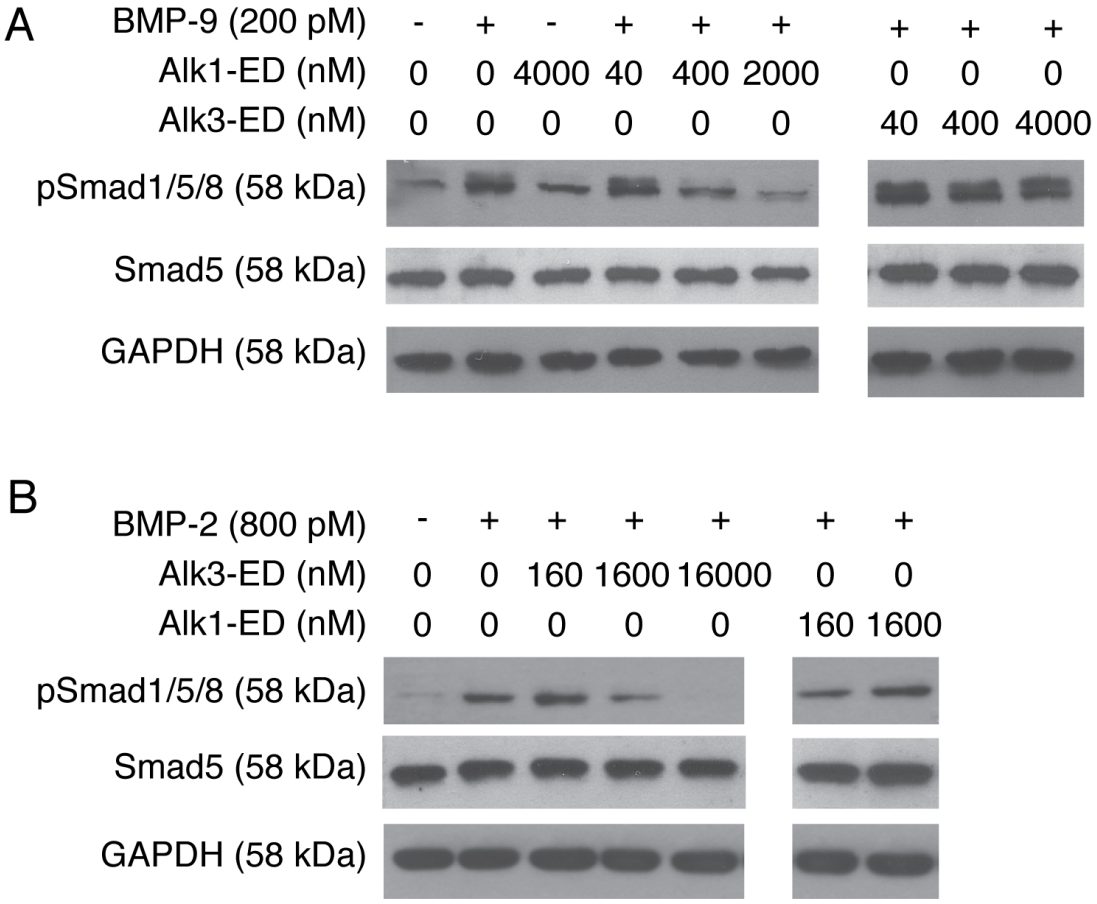
A
BMP-9 (200 pM) - + - + + + + + +
Alk1-ED (nM) 0 0 4000 40 400 2000 0 0 0
Alk3-ED (nM) 0 0 0 0 0 0 40 400 4000
pSmad1/5/8 (58 kDa)
Smad5 (58 kDa)
GAPDH (58 kDa)
B
BMP-2 (800 pM) - + + + + + +
Alk3-ED (nM) 0 0 160 1600 16000 0 0
Alk1-ED (nM) 0 0 0 0 0 160 1600
pSmad1/5/8 (58 kDa)
Smad5 (58 kDa)
GAPDH (58 kDa)

Fig. 4

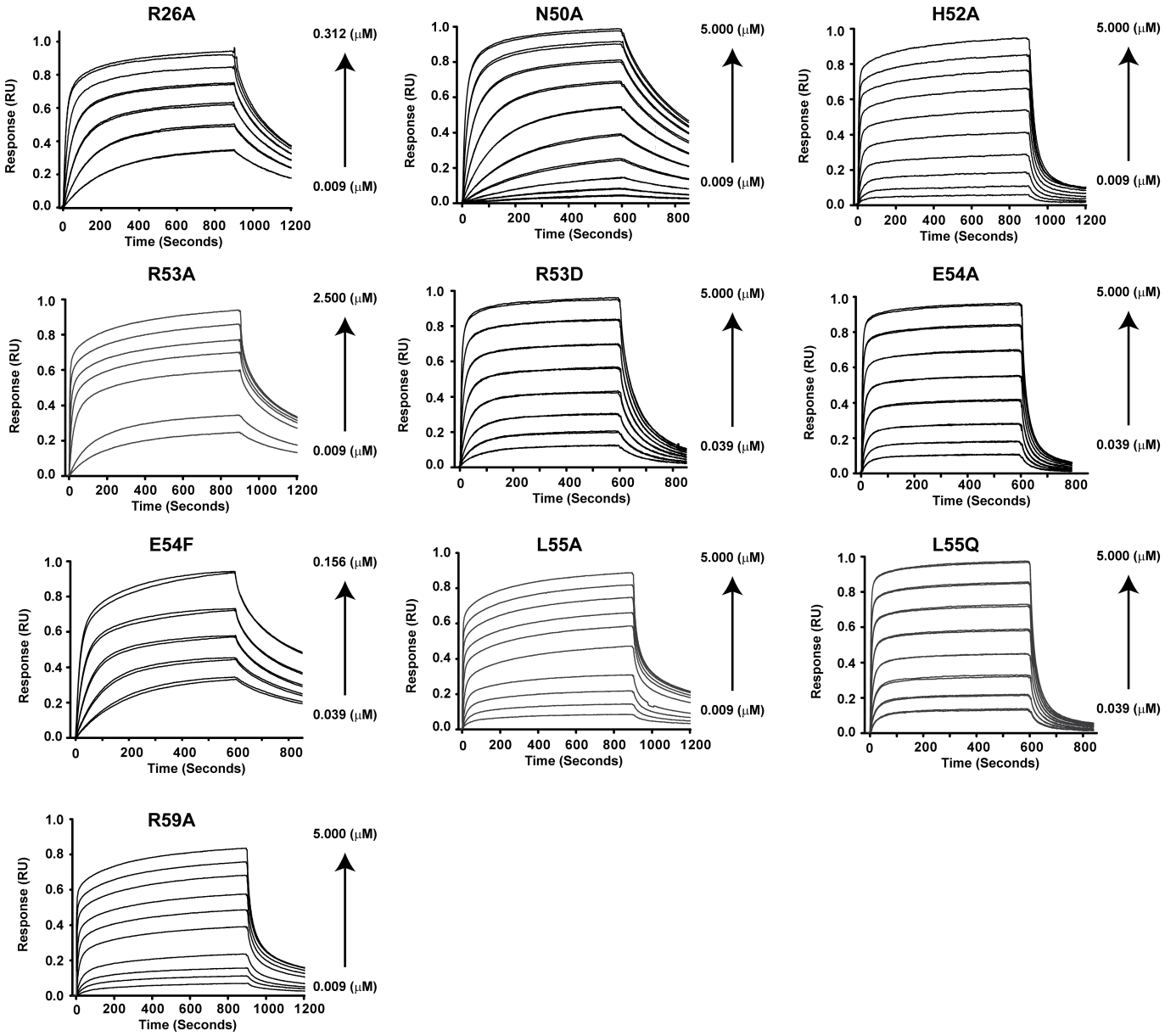
R26A
0.312 (μM)
0.009 (μM)
N50A
5.000 (μM)
0.009 (μM)
H52A
5.000 (μM)
0.009 (μM)
R53A
2.500 (μM)
0.009 (μM)
R53D
5.000 (μM)
0.039 (μM)
E54A
5.000 (μM)
0.039 (μM)
E54F
0.156 (μM)
0.039 (μM)
L55A
5.000 (μM)
0.009 (μM)
L55Q
5.000 (μM)
0.039 (μM)
R59A
5.000 (μM)
0.009 (μM)
Response (RU)
Time (Seconds)

Fig. 5

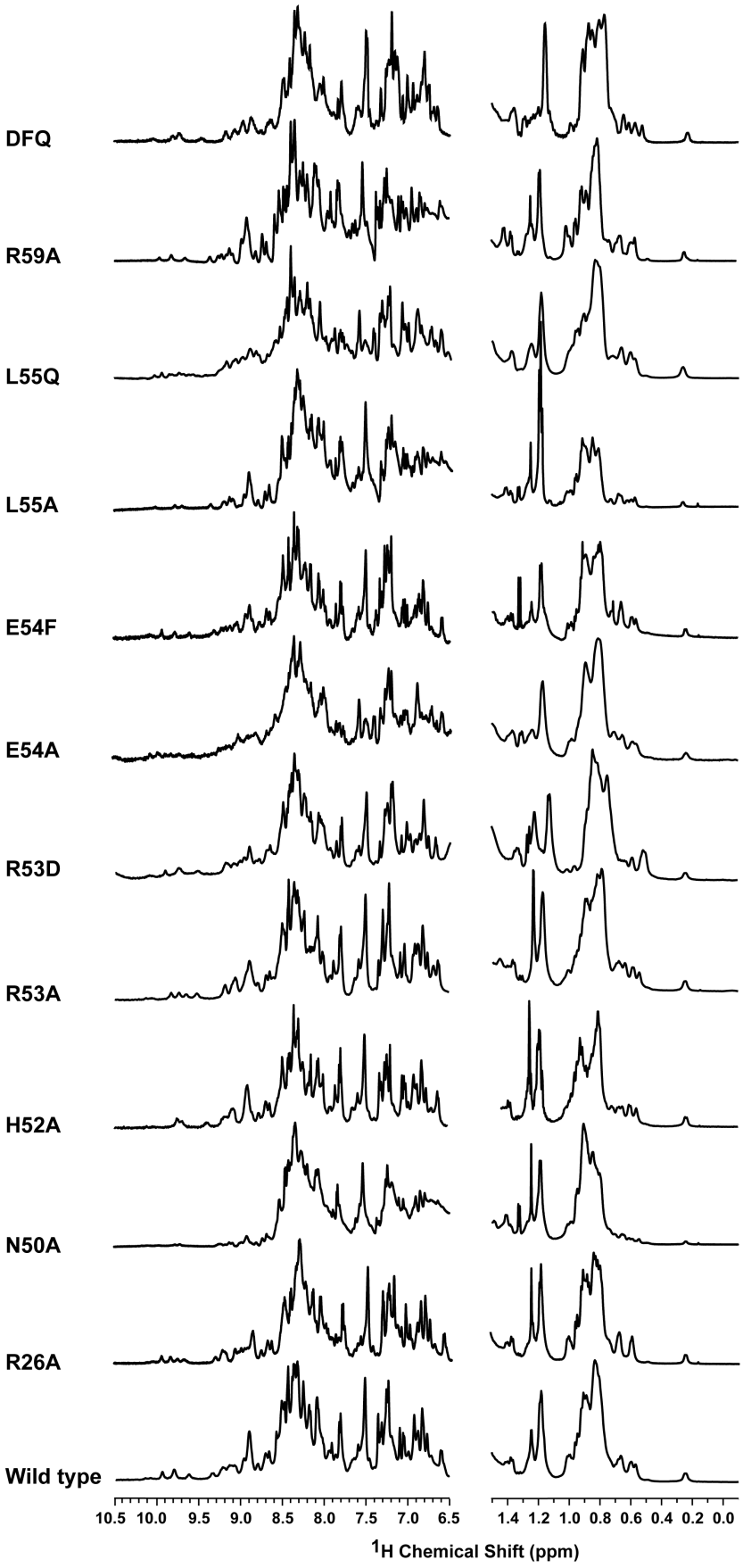
DFQ
R59A
L55Q
L55A
E54F
E54A
R53D
R53A
H52A
N50A
R26A
Wild type
10.5 10.0 9.5 9.0 8.5 8.0 7.5 7.0 6.5
1.4 1.2 1.0 0.8 0.6 0.4 0.2 0.0
1H Chemical Shift (ppm)

Fig. 6

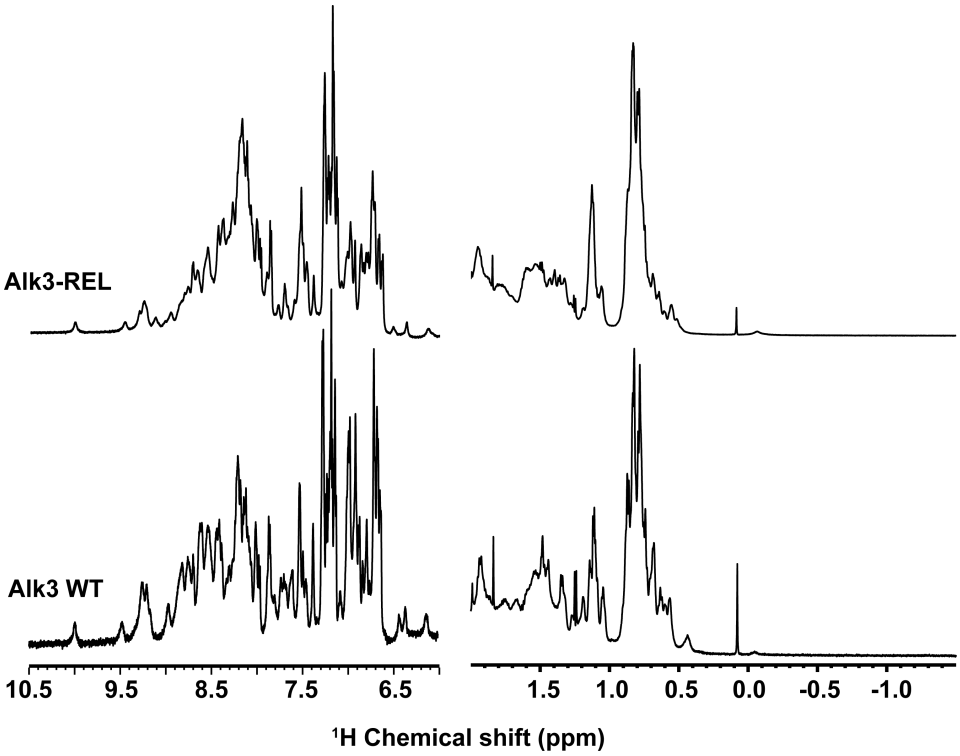
Alk3-REL
Alk3 WT
10.5
9.5
8.5
7.5
6.5
1.5
1.0
0.5
0.0
-0.5
-1.0
¹H Chemical shift (ppm)

Fig. 7

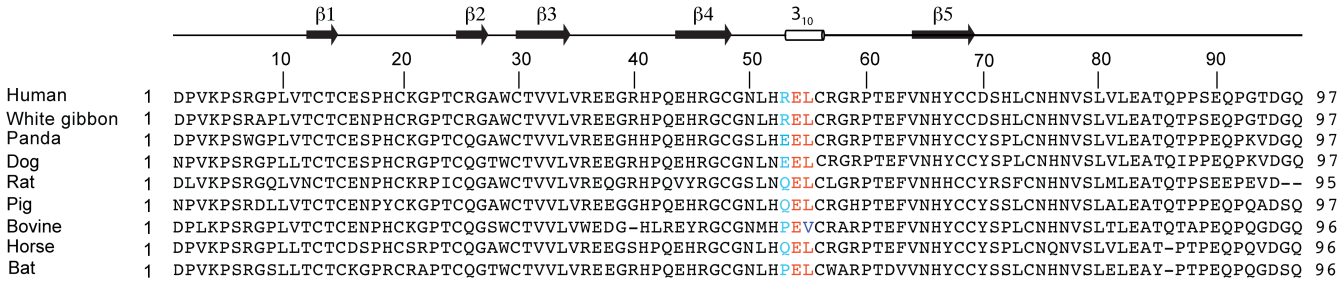
β1
β2
β3
β4
3₁₀
β5
10
20
30
40
50
60
70
80
90
Human 1 DPVKPSRGPLVTCTCESPHCKGPTCRGAWCTVVLVREEGRHPQEHRGCGNLHRELCRGRPTEFVNHYCCDSHLCNHNVSLVLEATQPPSEQPGTDGQ 97
White gibbon 1 DPVKPSRAPLVTCTCENPHCRGPTCRGAWCTVVLVREEGRHPQEHRGCGNLHRELCRGRPTEFVNHYCCDSHLCNHNVSLVLEATQTPSEQPGTDGQ 97
Panda 1 DPVKPSWGPLVTCTCESPHCKGPTCQGAWCTVVLVREEGHHPQEHRGCGSLHEELCRGRPTEFVNHYCCYSPLCNHNVSLVLEATQTPPEQPKVDGQ 97
Dog 1 NPVKPSRGPLLTCTCESPHCRGPTCQGTWCTVVLVREEGRHPQEHRGCGNLNEELCRGRPTEFVNHYCCYSPLCNHNVSLVLEATQIPPEQPKVDGQ 97
Rat 1 DLVKPSRGQLVNCTCENPHCKRPICQGAWCTVVLVREQGRHPQVYRGCGSLNQELCLGRPTEFVNHHCCYRSFCNHNVSLMLEATQTPSEEPEVD-- 95
Pig 1 NPVKPSRDLLVTCTCENPYCKGPTCQGAWCTVVLVREEGGHPQEHRGCGNLHQELCRGHPTEFVNHYCCYSSLCNHNVSLALEATQTPPEQPQADSQ 97
Bovine 1 DPLKPSRGPLVTCTCENPHCKGPTCQGSWCTVVLVWEDG-HLREYRGCGNMHPEVCRARPTEFVNHYCCYSPLCNHNVSLTLEATQTAPEQPQGDGQ 96
Horse 1 DPVKPSRGPLLTCTCDSPHCSRPTCQGAWCTVVLVREEGSHPQEHRGCGNLHQELCRGRPTEFVNHYCCYSPLCNQNVSLVLEAT-PTPEQPQVDGQ 96
Bat 1 DPVKPSRGSLLTCTCKGPRCRAPTCQGTWCTVVLVREEGRHPQEHRGCGNLHPELCWARPTDVVNHYCCYSSLCNHNVSLELEAY-PTPEQPQGDSQ 96

Fig. 8

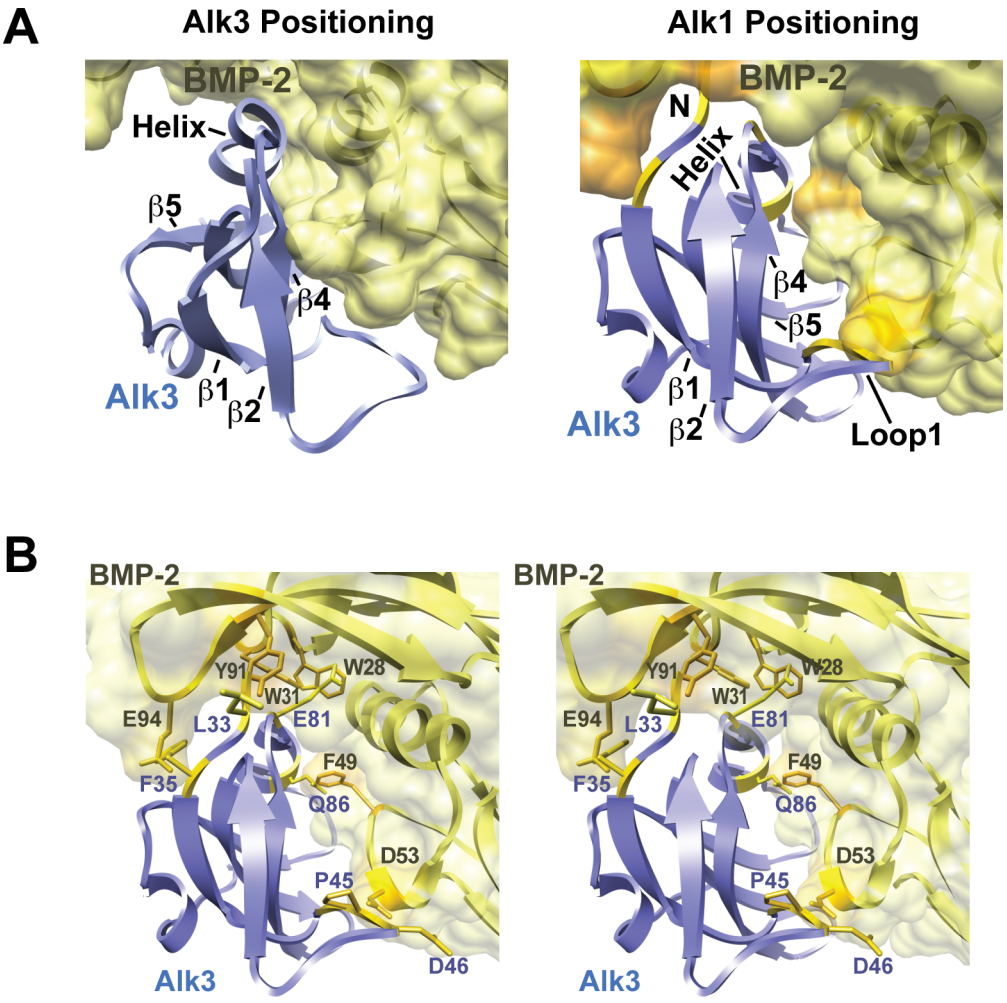
A
Alk3 Positioning
Alk1 Positioning
BMP-2
Helix
β5
β4
Alk3
β1
β2
BMP-2
N
Helix
β4
β5
β1
Alk3
β2
Loop1
B
BMP-2
Y91
W28
W31
E94
L33
E81
F49
F35
Q86
D53
P45
D46
Alk3
BMP-2
Y91
W28
W31
E94
L33
E81
F49
F35
Q86
D53
P45
D46
Alk3